

**OVER A QUARTER CENTURY of TCTOR:  
TROPICAL CYCLONE TORNADOES in the WSR-88D ERA**

Roger Edwards<sup>1</sup> and R. M. Mosier  
Storm Prediction Center, Norman, OK

## 1. INTRODUCTION and BACKGROUND

Tropical cyclones (TCs) effectively act as a category of organized mesoscale convective system (Spratt et al. 2008; Edwards 2012, hereafter E12), persisting for tens of hours to a few days during land-interaction stages over the central and eastern U.S., while producing tornadoes at highly variable rates (e.g., McCaul 1991; E12; Schenkel et al. 2020). Some produce no tornadoes—even if landfalling as mature hurricanes such as Kate in 1985 (Case 1986)—whereas others may spawn over 100 (Table 1). As with their midlatitude counterparts, TC tornadoes sometimes produce casualties (deaths and injuries), which justifies their explicit categorization and recording from a risk-assessment perspective.

Table 1: Updated version of Table 1 in E12—the top ten known TC-tornado counts—using SPC dataset of TC tornadoes (TCTOR) for TCs since 1995, Orton (1970) for Beulah, and NCEI *Storm Data* for Andrew.

<b>TROPICAL CYCLONE</b>	<b>YEAR</b>	<b>TORNADO REPORTS</b>
H Ivan	2004	118
H Beulah	1967	115
H Frances	2004	103
H Rita	2005	97
H Katrina	2005	59
H Andrew	1992	56
H Harvey	2017	52
TS Fay	2008	50
H Gustav	2008	49
H Georges, H Cindy	1998, 2005	48

Forecasting TC tornadoes has advanced over the past three decades beyond largely climatological and empirical concepts (Weiss 1987), to ingredients-based (Doswell 1987; Johns and Doswell 1992), cyclone-customized, situational diagnosis and predictive methods. Most occur in supercells, though a small minority of TC tornadoes has been

nonsupercellular (Edwards et al. 2012a). As such, the same basic ingredients used to diagnose and forecast tornadic supercell environments in midlatitudes (moisture, instability, lift sources, vertical shear) apply in TCs, just in differing environmental proportions (e.g., McCaul 1991; Edwards et al. 2012b; Schenkel et al. 2020). This shift in operational thinking recognizes that each TC presents its own spatiotemporally unique meso- to storm-scale tornado threats, both over the whole tornadic phase of a TC, and as an evolving system from day to day (e.g., Baker et al. 2009; Nowotarski et al. 2021). This manifests as differing counts and spatial distributions of tornadoes from one TC or TC day to another. Still, most tornadoes occur in the northeast to east sector (Edwards 2010, hereafter E10; and E12). That physically relates to the internal distribution of favorable CAPE and low-level shear (e.g., McCaul 1991, Molinari and Vollaro 2009) and in an overarching sense, to the influence of ambient deep-tropospheric shear on both the TC convective structure and buoyancy-shear parameter spaces (Schenkel et al. 2020).

While the National Hurricane Center (NHC) forecasts TC track, intensity, size (wind radii), storm surges, and issues TC watches and warnings, the Storm Prediction Center (SPC) is responsible for nationwide outlooks, mesoscale discussions, and watches for tornado potential within TCs. During imminent, landfalling and post-landfall stages of classified TCs, SPC and NHC coordinate the tornado forecasts (Edwards 1998; E12), now via a remote-video function, with affected local NWS forecast offices and regions. Examples of SPC forecast products, using formats current as of this writing, are shown in Edwards et al. (2018) for a relatively recent hurricane: Harvey of 2017. For more on SPC forecast formats and development, see Edwards et al. (2015).

As a part of decision-support services for TCs influencing their jurisdictions, local NWS forecast offices issue multihazard text bulletins, and web- and e-mail-based graphical products, for approaching and overhead TCs that include tornado threats (based largely on SPC outlooks). Those offices also issue tornado warnings when storm spotters and/or radars indicate a tornado is imminent or ongoing. The onset of dual-polarization capabilities in the early 2010s enabled theretofore impossible radar detection of tornadic debris signatures (Edwards and Picca 2016;

<sup>1</sup> *Corresponding author address:* Roger Edwards, Storm Prediction Center, National Weather Center, 120 Boren Blvd #2300, Norman, OK 73072; E-mail: roger.edwards@noaa.gov

Nowotarski et al. 2021) to aid in the warning, verification and damage-survey processes. Increasingly, TC tornado warnings are also informed by both SPC and local mesoanalytic insights (e.g., Edwards and Pietrycha 2006; Nowotarski et al. 2021), not just radar characteristics. An evolutionary perspective on local warning issues for TC tornadoes, through the “modernized” NWS’ WSR-88D era, can be gained via combined reading of Spratt et al. (1997), Schneider and Sharp (2007) and Nowotarski et al. (2021).

Despite advances in operational prediction of TC tornadoes, their climatology still forms an important basis for understanding their bulk distributions—whether across yearly to decadal timespans, geographically, or from the frame of reference of the TC center. Consistently derived, accurate TC-tornado climatology and case data can inform not only operational forecasting, but broader climatic studies (e.g., Carroll-Smith et al. 2021), numerical modeling work (e.g., Carroll-Smith et al. 2019), and general risk analysis akin to those with ONETOR (Schaefer and Edwards 1999). Following earlier TC-tornado climatologies (e.g., Pearson and Sadowski 1965; Hill et al. 1966; Novlan and Gray 1974; McCaul 1991; Verbout et al. 2007; Schultz and Cecil 2009), E10 introduced the SPC TC tornado dataset (TCTOR), as a consistently, meteorologically derived climatology common to the WSR-88D era. This work is a follow-up, with an additional 12 years of data and results, as well as newer analyses and display techniques.

## 2. DATA CHARACTERISTICS

The TCTOR dataset contains both individual-tornado information and corresponding entries on strength and central position of their TCs at tornado time. The dataset is flexible, in that existing entries may be amended at any time, with documentation in “readme.txt”, as errors or newer information are discovered on events. E10 documented the original TCTOR process in detail, which is summarized and updated in this section.

### a. Tornado records

Each year’s finalized listing of tornadoes from the SPC national dataset (Schaefer and Edwards 1999) becomes available following the end of Atlantic hurricane season, usually in the first few months of the following year. Those data are known as “one tornado” (ONETOR) because they represent conjoining of *Storm Data* county segments for those paths that cross county lines. As such, ONETOR represents single-path data for each known tornado nationally. For TCTOR, we additionally conjoin paths crossing state lines, while noting that condition in the “state” column of the data. During years when delays exist in yearly ONETOR finality, TCTOR may be prepared using stitched *Storm Data* county segments, in a similar process to ONETOR, then cross-checked with the latter once the fuller national data are final.

Those ONETOR or *Storm Data* reports that appear to occur in or near TCs are examined individually, on a yearly basis, as candidates for inclusion in TCTOR. Using fixed TC-center-relative

radii as inclusion criteria (e.g., numerous historic climatologies referenced in E12) is expedient for automated processes, but fails to account for variations in TC size from day to day and cyclone to cyclone. Recent research (Paredes et al. 2021) has shown that TC size matters with respect to tornado distribution and frequency (larger TCs generally yielding more tornadoes), further justifying a TC-individualized approach. TCTOR records therefore depend on more time-intensive human meteorological analyses. A TCTOR event must occur within the circulation envelope of either a classified TC or its remnant inland low, as long as the low-level cyclone still resides under warm-core midtropospheric conditions. In most cases (>95% of events), this is readily apparent from satellite and/or composite radar imagery, along with surface and upper-air observational charts commonly available in SPC operations and online archives. Such tornadoes also are usually explicitly and independently denoted as TC tornadoes in commentary accompanying NCEI *Storm Data* records. These include tornadoes within TCs that occur in surface baroclinic zones of any origin (Edwards and Pietrycha 2006).

The remaining tornadoes, constituting spatiotemporal fringe events, are plotted manually with respect to surface and upper-air analyses to determine that each occurred in a low-level cyclone, beneath the remnant warm core or midtropospheric thermal ridge from the previously classified TC. A disqualified tornado example would be one occurring along a frontal zone well-removed from its interaction with a TC. Another would be a tornado occurring near a frontally merged, formerly tropical low, but beneath the cyclonic-flow field and cooling midlevel temperatures related to an approaching midlatitude shortwave trough. Tornadoes also have been excluded within tropical air masses left behind TCs, in ensuing days, but after the departure or dissipation of the closed cyclone. Tornadoes associated with either open-wave surface troughs, weak tropical or subtropical lows, or midlatitude convective complexes that *later* became classified TCs, also are excluded.

The inclusion of 2021 data into TCTOR records represents 27 years of data, with 1746 events since 1995. Counts of TC tornadoes and tornadic TCs can differ greatly from year to year (Fig. 1). Individual TCs produce tornadoes at variable rates; therefore, yearly tornado counts do not necessarily follow the trends in tornadic TCs. ONETOR also has all known TC tornadoes before 1995. However, that year marked the conclusion of a substantial shift in NWS warning and verification practices concurrent with the essentially finalized deployment of the WSR-88D network across TC-affected areas (E10; E12). A change from mean to max path width for data entry also occurred in 1995 (Edwards et al. 2021). The combined effects of the early- to mid-1990s changes represented a systemic data “shock” (Thorne and Vose 2010) to tornado recordkeeping that manifest in absolute tornado numbers, both nationwide and in TCs (e.g., Verbout et al. 2003, 2007; E12). Figure 2 illustrates this. The years approaching 1995 also represented the relative appearance of TC tornadoes in different damage-rating bins (E12) on the Fujita (1971) and Enhanced Fujita (EF) (Doswell et al. 2009;

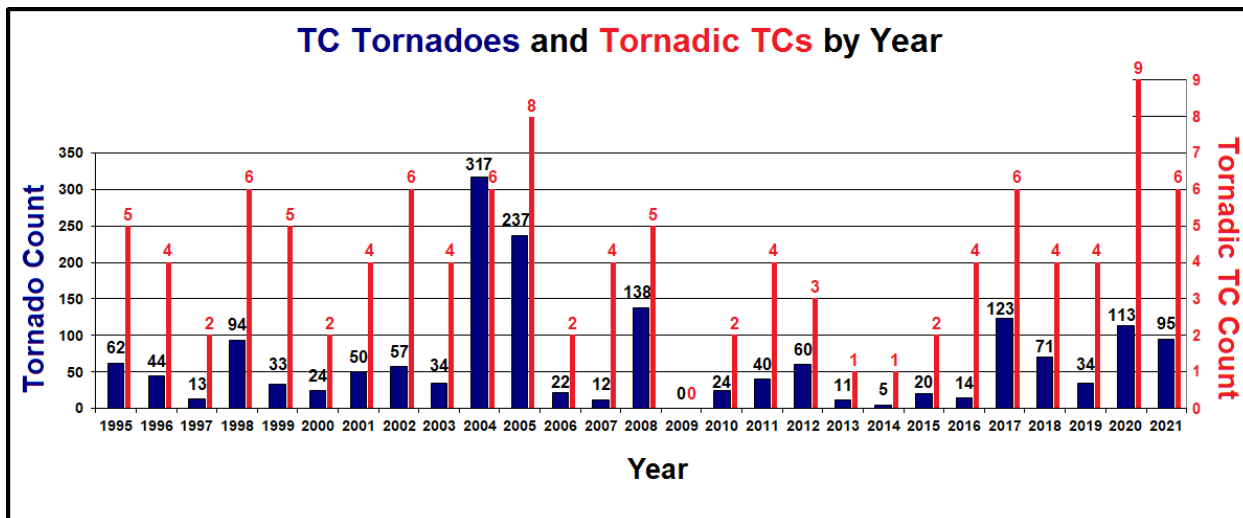


Figure 1: Counts of tornadoes (blue, left ordinate) and tornadoic TCs (red, right ordinate) for each year of TCTOR (abscissa).

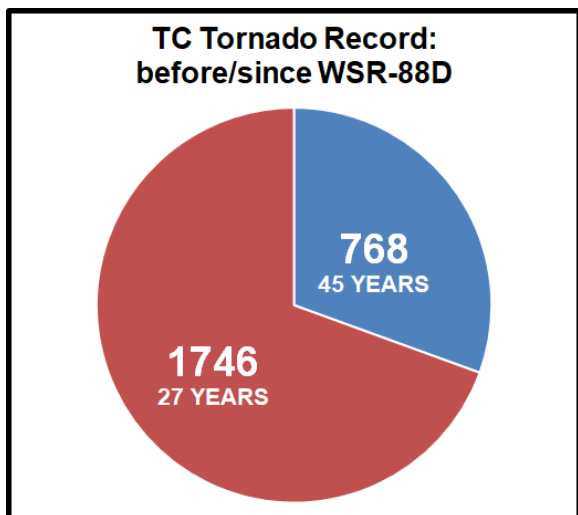


Figure 2: Tornado counts in blue derived from ONETOR prior to 1995 by Schultz and Cecil (2009), and from TCTOR since (red), illustrating the influence of modern tornado detection, warning and verification practices on the data.

Edwards et al. 2013) scales, with more weak (F0–F1) events being recorded concurrent with warning-verification efforts related to the WSR-88D operationalization.

#### b. Data format

The final TCTOR dataset is maintained in Microsoft Excel™ format, due to its ubiquity, ease of color-coding for event-tracking's sake, and ready convertibility to more universal formats (such as comma-separated value) used across operating systems and hardware platforms. A plain-text file that accompanies TCTOR, "readme.txt", provides specific column-based documentation of the data, a reverse-chronological listing of yearly data updates, and lists any intervening additions, deletions, corrections, amendments, and format changes performed since TCTOR's inception. This permits cross-checking by

researchers across versions, for reproducibility's sake, and to determine the cause of minor changes in analytic results that can occur in the same data subsets across TCTOR versions. Both tctor.xls and readme.txt are public-domain files, freely available from the authors.

Among the format changes since E10 is the addition of a column for each tornado's destruction potential index (DPI; Thompson and Vescio 1998), which is computed directly from the path length, maximum width, and damage rating already available in ONETOR. This is the only purely tornado-specific information (not related to TC characteristics) in TCTOR that ONETOR does not contain. A ONETOR column representing yearly tracking number has been removed from TCTOR since E10, because of irrelevance and disuse.

#### c. TC tracks and intensities

To determine tornado timing and location with respect to TC position and motion, and to bin tornadoes by classified TC intensity at ONETOR tornadogenesis time, TCTOR incorporates data from the NHC HURricane DATaset, second version (HURDAT2, Landsea and Franklin 2013). HURDAT2 data are standardized according to documentation for the International Best-Track Archive for Climate Stewardship (IBTrACS; Knapp et al. 2010). These data include each TC's six-hourly strength (by pressure and maximum sustained wind), along with contemporaneous latitude and longitude fixes of the cyclone center, matching those initially presented in tabular form in NHC single-TC event reports.

TC central latitude, longitude, pressure, and peak intensity from HURDAT fill columns in TCTOR, along with digital representations of classification category (5 for category 5 hurricanes, down to 0 for tropical storms, -1 for tropical depressions, and -2 for remnant lows), and interpolated center positions at tornado time. Even if a TC's center did not reach the conterminous U.S. (e.g., a center path just missing

the Atlantic Coast, or a landfall in northeastern Mexico), its U.S. tornadoes are included in TCTOR (Fig. 3). In the improbable event that any eastern Pacific TCs survive long enough to produce tornadoes in the Southwest, those would be included as well.

For timeliness, the NHC online TC reports may supply “early HURDAT2” data for TCTOR. Though rare for tornadic TCs documented so far, any discrepancies between TC-report data and final HURDAT would be corrected and included as revisions in TCTOR, and specified as such in the accompanying “readme.txt” news file. The spherical-geometry method used to compute center-relative azimuth and range of reported tornadogenesis points was detailed in E10 and has not changed. Other techniques, such as interpolation using a piecewise cubic Hermite polynomial (e.g., Schenkel et al. 2020), may yield center-relative position differences ~1–10 km compared to native TCTOR calculations, but would not affect bulk patterns herein substantially.

### c. Potential sources of error and uncertainty

Some of the same potential sources for tornado-path error in the *Storm Data* at large (Edwards et al. 2022, this conference) sometimes may evade initial quality control to affect TCTOR, including:

- Typographical errors (including extra or missing digits in path length and width),
- Mistaken local entries of one path characteristic as another,
- Zeroes for path length or width,
- Length less than width,
- Offsets between Storm Data segments,
- Time-offset mistakes (including time-zone conversion errors),
- Recording of later report-receipt times as tornado-occurrence times, and
- Tornado times and/or locations displaced from associated radar echoes.

Examples of each such error type have been found in TCTOR quality control, which includes coordination of resulting *Storm Data* revisions with local warning-coordination meteorologists. Several researchers who have used TCTOR (see Acknowledgments), as well as the authors, also have discovered such errors in post-production TCTOR analysis. Documented errors are fixed in TCTOR and Storm Data, then submitted to ONETOR for reconciliation, and are documented in “readme.txt”. Other errors still may exist in the data, including unknown errors such as undetected subtle mistakes in data entry, and those arising from the undersampling and subjectivity of the damage-rating process (Doswell and Burgess 1998; Doswell et al. 2009; Edwards et al. 2013). The authors welcome submissions of research-based TCTOR corrections, with documentation.

As with ONETOR, unknown or hidden tornado errors are possible, but not quantifiable. These include either missing or extra, misreported weak tornadoes whose evidence is obscured by the TC itself. Misreported tornadoes have been a suspected

but unprovable cause of some TC tornado records accompanying nonsupercellular radar-assessed convective modes (Edwards et al. 2012a). Unavoidable path-definition uncertainties for recorded tornadoes exist in areas that are remote, inaccessible to surveyors, devoid of damage indicators, or also affected by intense gradient-wind or hydraulic damage from the TC. Position and time errors also may exist where radar-based corroboration is unavailable or has not been performed yet. ONETOR and TCTOR path lengths represent straight lines between documented start and end points. As such, given that tornado tracks can curve, *path length represents the minimum value for each tornado*.

Errors also may exist in HURDAT itself (Torn and Snyder 2012; Landsea and Franklin 2013), and by extension, in tornado azimuths and ranges measured from geometrically interpolated TC center positions. The latter may arise from uncommon but possible rapid accelerations or decelerations between 6-hourly fixes, introducing uncertainty. HURDAT positions truncate to the tenth of a degree of latitude and longitude, at least an order of magnitude coarser than most *Storm Data* tornado positions. Center fixes for mature hurricanes near the coast are the most certain, given the presence of an eye on radar(s). Decaying and/or poorly organized TCs (generally tropical depressions or post-classification lows) carry the most central-position uncertainty, especially if located in areas of sparse surface observations, satellite-observed dense overcast, and/or poor low-level radar coverage. All studies and climatologies using TC-relative tornado positions contain these TC-related uncertainties. As such, TC-relative tornado positions should be treated as approximations, regardless of analytic numeric precision to the km or finer resolution. Finally, tornado-data analyses, in general, become more uncertain and error-prone with shrinking sample size (Doswell 2007).

### 3. MAPPING and ANALYSES, 1995–2021

Data analyses from E10 have been updated to include TCs through 2021; the data also will be examined in additional ways throughout this section. This is intended to be a summary coverage, as the potential permutations of sorting and presentation of TCTOR data are practically limitless. Here are some “quick facts” on the full 1995–2021 TCTOR:

- Fatalities recorded: 29
- Injuries recorded: 403
- Most from one TC: 118 (Ivan-2004)
- Most-active year: 2004 (317)
- Least-active year: 2009 (0)
- Average per year: 64.7
- Highest damage rating: F/EF3 (5 events)
- Longest path: 52 mi (83.7 km), 1530 UTC 7 October 1996, DeSoto/Hardee/Polk Counties, FL, TC Josephine
- Average path length: 2.37 mi (3.8 km)
- Widest path: 1000 yd (914 m), 0419 UTC 17 September 2018, Sampson County, NC; TC Florence
- Average path width: 85.2 yd (77.8 m)
- Average DPI: 0.44



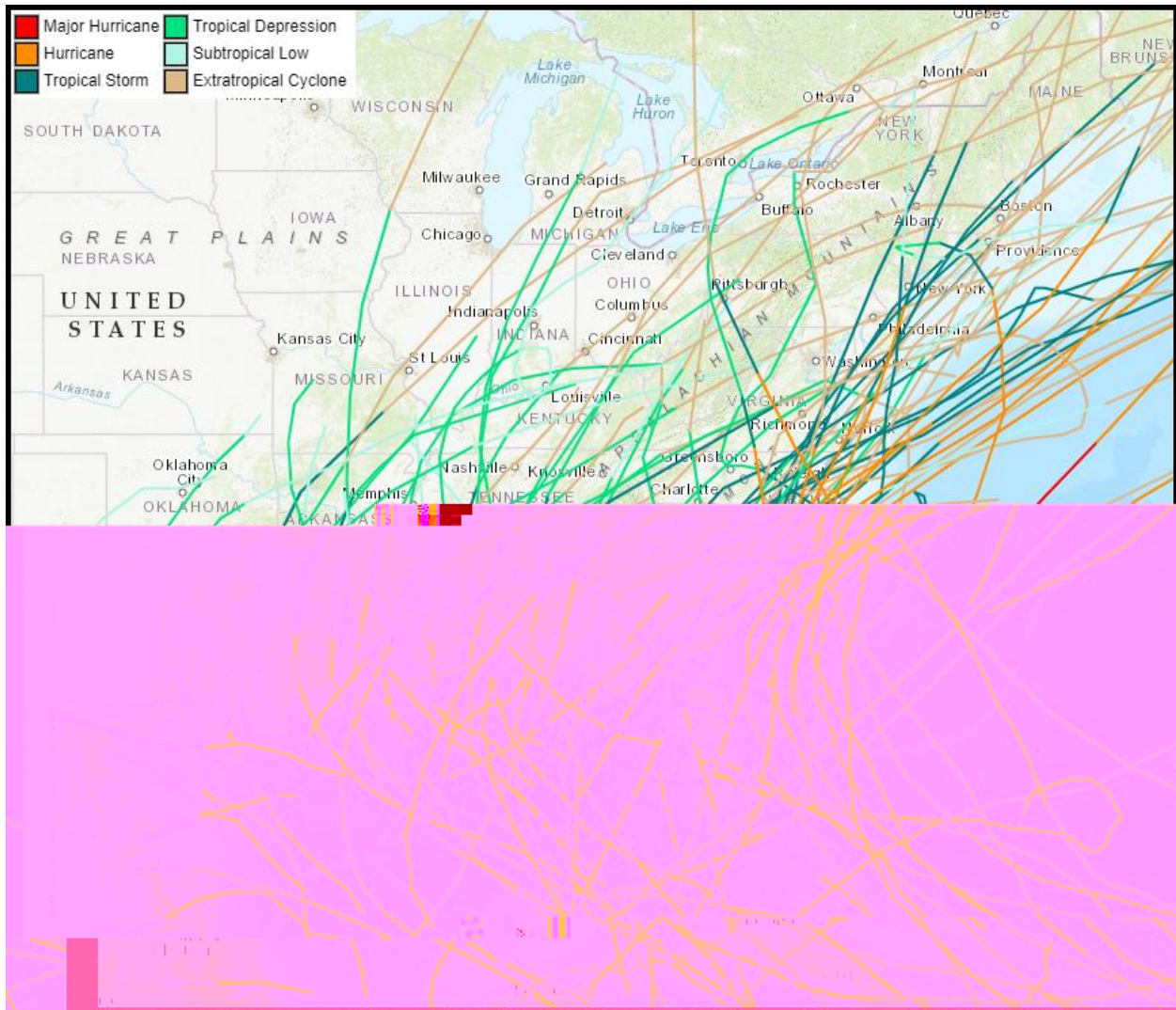


Figure 3: Tracks of tornadic TCs in the conterminous U.S. (CONUS), 1995–2021, including pre- and post-tornadic stages. Classified intensity (or extratropical stage) is color-coded for each TC according to legend at upper left.

- Largest DPI: 31.95, 2040 UTC 31 August 2017, Pickens/Lamar/Fayette Counties, AL, TC Harvey
- Deadliest tornado: 4 killed, 0207 UTC 16 September 2004, Calhoun County, FL; TC Ivan.
- Average classified TC windspeed at tornado time: 50 kt ( $25.7 \text{ m s}^{-1}$ ) tropical storm
- Average TC central MSL pressure at tornado time: 985.5 hPa

a. Geography

TCTOR events concentrate within 500 km of the Gulf and Atlantic Coasts, but have occurred as far inland as Oklahoma, Missouri and the Ohio Valley States, and as far north as Maine (Fig. 4). The sampling period straddles the early 2007 transition from nominally cross-calibrated Fujita (F) and Enhanced Fujita (EF) damage scales (Edwards et al. 2013). Significant tornadoes rated F/EF2 or greater (Hales 1988) are somewhat more common over Florida and the Atlantic Coast States than the Gulf Coast States.

The top five TCTOR state counts are: Florida (370), North Carolina (221), South Carolina (187), Alabama (157), and Mississippi (152). Arkansas (41) had the most in a landlocked state. Tornado production decreases: 1) gradually northward because of TC degradation, extratropical transitions and more-limited instability, and 2) sharply westward from about  $98^\circ$  west longitude, due to fewer TC paths and decreasing moisture. TC-tornado frequency over water is unknown, though dropsondes have indicated favorable offshore environments (Molinari and Vollaro 2010), and strong TC supercells have been detected at sea (e.g., Spratt et al. 1997; Eastin and Link 2009). Figure 2 of E12 is a photograph of a supercellular waterspout near Key West, FL, from Hurricane Wilma (2005).

b. TC intensity and classification

Most TC tornadoes occur at less than classified hurricane intensity, with tropical storms representing (by a small margin) the greatest tornadic production stage of the TC lifecycle (Fig. 5). No TC tornadoes

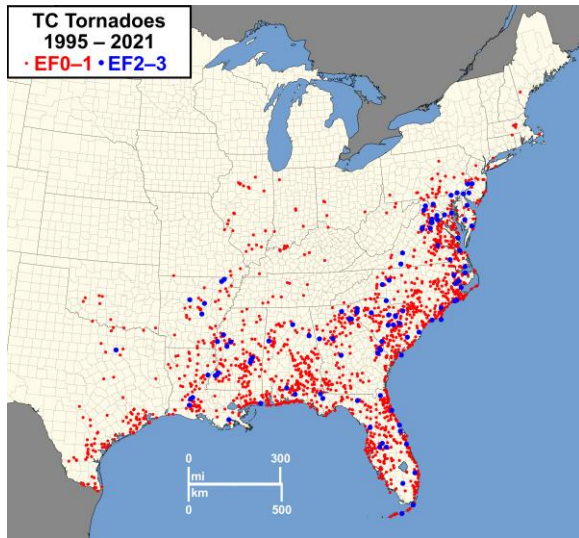


**Figure 4:** TCTOR start-point map for all areas affected in the conterminous U.S., 1995–2021. Weak (F/EF0–F/EF1) rated tornadoes, in red, significant (F/EF2–F/EF3) in blue. Some events overlap at this scale. No F/EF4–F/EF5 tornadoes occurred. Mapping by Matt Elliott.

have occurred from category-5 hurricanes since the four reported by E10, decreasing the overall percentage in that bin to 0.2%. This is a manifestation more of the lack of such systems at or near landfall than any inability of theirs to spawn tornadoes, though the one category 5 landfalling TC so far in the EF era—Michael of 2018—waited until weakening to category 4 to become tornadic. Major hurricanes (category 3–5 in aggregate) produced 165 tornadoes, about 36% of all tornadoes from hurricanes, and 9.4% of all TCTOR records.

The preponderance of sub-hurricane TCs in the tornado record (73.5%) reflects both their overall commonality as landfalling and inland systems, and the decreasing overwater coverage of supercell-favoring sectors as the TCs penetrate inland. By contrast, mature hurricanes tend to still have substantial overwater coverage, decreasing spatial opportunity for tornado reports. This geographic limiting phenomenon should be taken into account when using center-relative TC-tornado distributions presented in the next subsection.

### c. Center-relative tornado distributions

One common way to evaluate tornado production by TCs—both in bulk and in individual cyclones—is by azimuth and range with respect to the interpolated TC center position at tornado time. In the literature, polar-plot analyses have been done mainly from three relative frameworks: true north, TC-translation direction, and more recently, the ambient deep-shear vector derived from numerical-model reanalysis data (Schenkel et al. 2020). The latter is more useful for operational forecasting purposes, and largely explains the other two from a physical perspective. With environmental analysis outside the scope of this paper, we will plot and compare north- and motion-relative frameworks in this subsection, given their

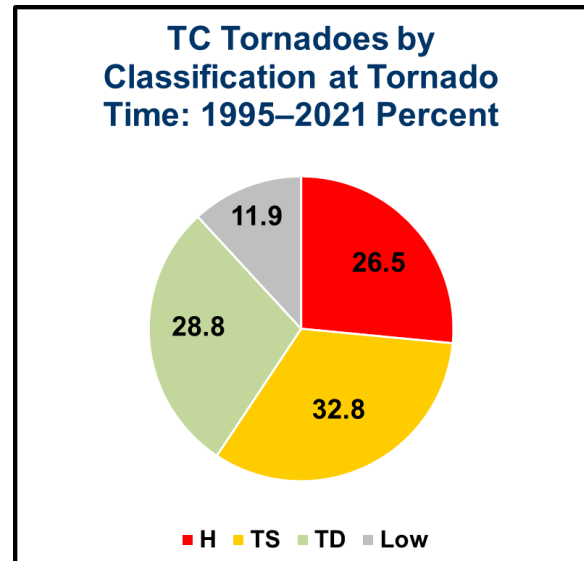


**Figure 5:** 1995–2021 TCTOR percentages by NHC and post-NHC classification at tornado time, using HURDAT’s Saffir-Simpson wind category (Schott et al. 2010; Simpson 1974) at tornado time. H is hurricane; TS is tropical storm; TD is tropical depression; “Low” (marked “N” in columnar TCTOR) includes all post-classification forms of tropical low.

decades-long familiarity from both E10 and the numerous published climatologies listed in E12.

Plotted from both the north-relative and TC-translation-relative frameworks, tornadoes show a strong preference for the eastern and right semicircles, respectively (Fig. 6). However, the polar distribution for translation-relative tornado locations shows more spread, largely from TCs moving with any southward- or westward-directed component (not shown), contrary to the prevailing southwesterly to westerly flow that typically influences TC recurvature at U.S. mainland latitudes. TCTOR events are most prevalent in the northeast quadrant (67.7%), followed by southeast (27.1%), with much fewer in the northwest (4.5% and southwest (0.7%). As in E10, the more concentrated scatter in the Fig. 6 radial plots from TCTOR still resemble the Schultz and Cecil (2009) distributions more than those of the more scattered McCaul (1991) climatology. The reason for the difference is unknown, but may relate to the years of overlap between the Schultz and Cecil (2009) data and early TCTOR, and/or the influence of more intensive WSR-88D report-gathering and warning-verification practices not relevant to the McCaul (1991) data.

Mainland U.S. tornado reports tend to shift clockwise and somewhat outward through the eastern semicircle as the cyclones weaken (Fig. 7). This characteristic long predates the WSR-88D era, as documented in Weiss (1987). Because of the absence of tornado reports (not necessarily actual tornadoes) over water, this effect is partly related to positioning of most or all of the tornado-favorable southeastern sector over the Gulf or Atlantic in pre-landfall to slightly post-landfall TCs (E10). However, a rightward and outward shift of tornadoes since has been documented relative to the deep-shear vector,

even for inland systems (Schenkel et al. 2020). Since the deep-shear vector is usually east of true north, this translates to a physically based rightward and outward influence on the Cartesian framework as well. Still, their shear-relative framework misses all of the tornadoes over water that preferentially would occur rightward (southeast) of the shear vector.

Tornado distributions can be strongly nonuniform from one TC to another, even as they aggregate into the bulk patterns shown in Figs. 6 and 7. Put another way, each TC leaves its own unique “tornadic footprint” relative to azimuth and range (e.g., Fig. 8). This footprint is regulated by the overlap of favorable environmental conditions (e.g., CAPE, large low-level hodographs) with the presence of sufficiently intense convection, usually as supercells (McCaul 1991; Edwards et al. 2012b; Schenkel et al. 2020). Nonsupercellular tornado reports in eyewalls and within a few km of TC centers are more poorly documented and dubious in nature, as discussed in more detail by E12.

*d. Comparisons with tornadoes nationwide*

Tornado reports were gathered concurrently from the nationwide database, as a part of the Edwards et al. (2022) work in this conference, and filtered similarly to TCTOR for optimal comparison. That filtering included consolidation of each state-line-crossing path to one tornado, via removal of single-state segments, and yielded 32775 reports, including those from TCs. TC tornadoes accounted for 5.3% of all tornadoes in the conterminous U.S.

Base variables commonly used to compare tornado events or occurrences include damage rating, path length, maximum (starting in 1995) path width, and human casualties (deaths and injuries). As estimated via damage rating, TC tornadoes tend to be weaker than the rest, with about 93% rated F/EF0–1 (Fig. 9). Significant ( $\geq$ F/EF2) tornadoes accounted for nearly 11% of all tornado reports, but only about 6% of TC tornadoes. EF-unknown has been little-used, with just six TCTOR records, all since 2019. Path length and width distributions (Figs. 10 and 11 respectively) show that TCTOR paths tend to be somewhat narrower and shorter than tornadoes as a whole, but only across the upper halves of the distributions. This mainly could reflect the relative lack of strong and especially violent (F/EF4–5) tornadoes in TCs, since tornadoes have longer and wider tracks overall with increasing rating (e.g., Brooks et al. 2004).

Using the initial, E10 version of TCTOR, Moore and Dixon (2012) assessed casualty information through 2009. Casualty records are summarized and updated here to include the ensuing 17 years. TC tornadoes accounted for 1.5% each of total national tornado deaths and injuries during the same period, despite being 5.3% of total tornado count. Their lesser rate of casualties may be attributed to generally shorter and narrower paths (Figs. 10 and 11)—offering less opportunity for encountering inhabited structures—and general tendency to produce weaker damage when they do (Fig. 9), compared to all tornadoes. For this purpose as well, TC tornadoes lack the violent, large-area tracks responsible for most national tornado casualties. Nonetheless, as potentially deadly aspects of tropical cyclones that

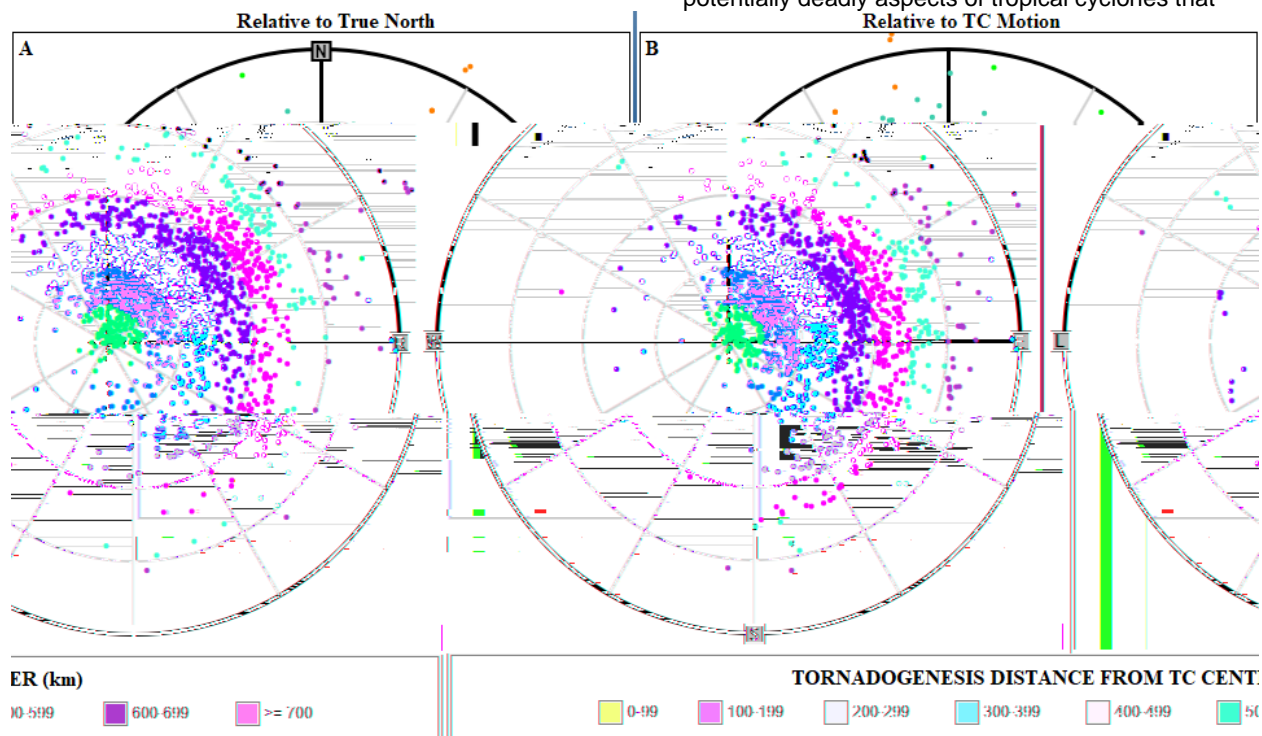


**Figure 6:** Polar graphs of TCTOR entries from 1995–2021 from center (plot origin), in the frameworks relative to: a) true north, b) TC translation direction at tornadogenesis. Range rings at 200-km intervals, radials at 30° intervals. Color coding (legend) further segregates distances into 100-km-wide annuli. Graphics generated using the online system described in Mosier and Edwards (2022, this conference).



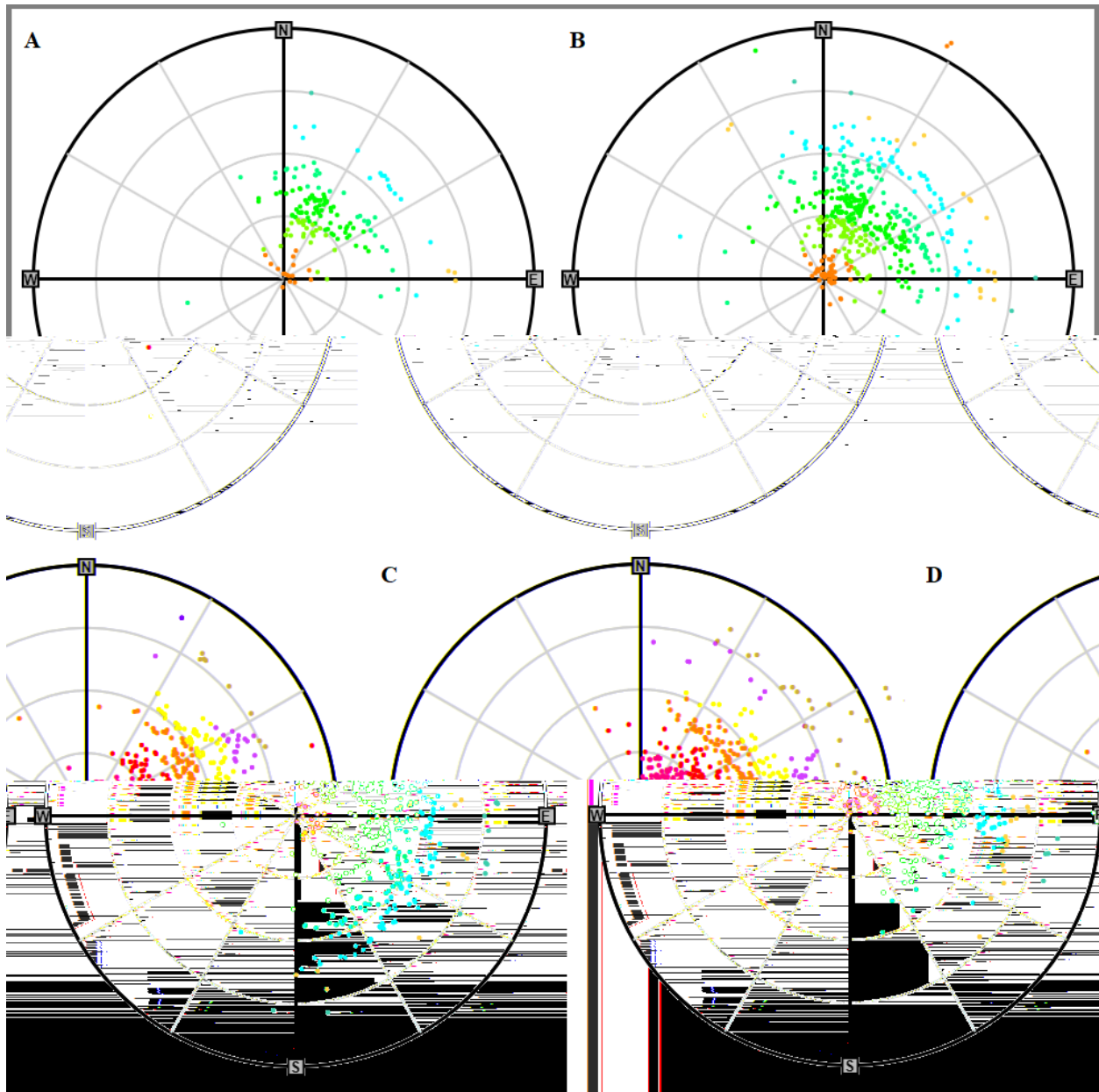


**Figure 7:** As in Fig. 5, but for these north-relative TC classifications valid *at tornado start time*: a) major hurricanes (category 3–5), b) all hurricanes, c) tropical storms, and d) tropical depressions and remnant lows.

typically occur away from the greatest core winds and storm surge (e.g., Figs. 5–7), tornadoes warrant careful attention in TC safety and preparedness efforts that typically focus closer to center.

*e. TC classification relative to radial distance*

Mean tornado distances from center were analyzed with respect to latitude and cyclone classification. Latitudinal bins of 5, beginning at 20° (with none lower than 21°), and ending with ≥40° (not shown), exhibited little variability in mean tornado radii from center between 299–314 km, except for a peak of 413 km when TC centers were between 20°–25° north. However, low TC and tornado sampling in that bin, and distance south of major U.S. landmass for much of the TC envelopes at those latitudes, may inflate the radial values.

For TC intensity comparisons, tropical depressions and remnant lows were binned together, since their central pressures and max windspeeds tended to intersperse. The one named tornadic subtropical storm (Lee of 2011) was grouped with tropical storms, being of the same lower-bound windspeed (35 kt, 18 m s<sup>-1</sup>). Figure 12 shows a decrease in mean tornado distance from the TC center with stronger TC classification. This may manifest the results of Schenkel et al. (2020), who found an outward spreading of tornadoes from center with stronger ambient deep-tropospheric shear (generally associated with less-organized TCs).

Since 95% of TC tornadoes occurred in the eastern semicircle, we focused there to determine if mean tornado distance from TC center varies with azimuth. The eastern half of the TC envelope was subdivided into six 30° bins (Fig. 13). Tornado



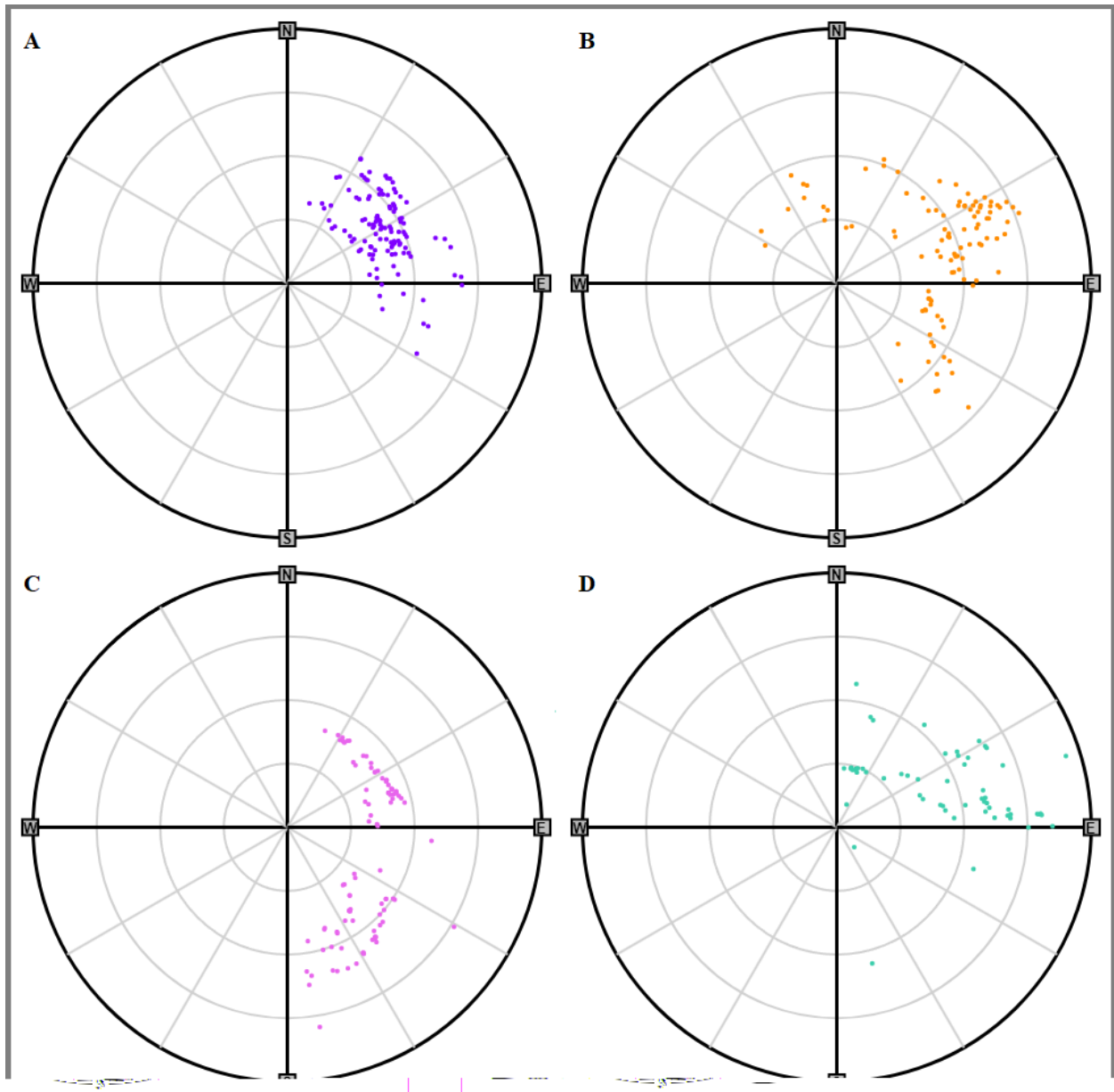


**Figure 8:** As in Fig. 6, but color-coded by TC for the top four TCTOR-era systems from Table 1: a) Ivan (2004, purple), b) Frances (2004, yellow-orange), c) Rita (2005, pink), and d) Katrina (2005, green-blue).

distance from center, on average, increased with clockwise curvature through the northeast quadrant, then varied in the southeastern quadrant, but at generally higher radii than to the northeast.

*f. Change from F to EF scales*

The change from F to EF rating occurred between the 2006 and 2007 hurricane seasons. The F era only included 44% of the TCTOR timeline herein, but contained 987 (56.5% of) TC tornadoes, largely due to the anomalously active years of 2004 and 2005 (Fig. 1). The EF scale had substantial bulk influences on tornadic path widths nationally (Edwards et al. 2021), with minor shifts in path lengths and damage ratings. However, for our TCTOR sampling, the F and EF eras had nearly identical path-width

distributions (not shown), with matching path widths at the 25<sup>th</sup>, 50<sup>th</sup> (median), 75<sup>th</sup>, and 90<sup>th</sup> percentiles, and a difference of just 5 m (18 for the F era, 23 for EF) at the 10<sup>th</sup> percentile. Path lengths for F vs. EF eras at all the same percentiles either were identical, or differed by  $\leq 0.1$  km—not statistically significant, and within the margin of error for length measurement. This shows that *non-TC tornadoes* were responsible for the EF-related significant gains in width, and lesser growth in length, documented by Edwards et al. (2021). How much of this lack of TCTOR influence on bulk national path trends is related to specialized TC environments, the overall smaller size, weaker damage and shorter lifespans of TCTORs, any systematic surveying differences, inherent imprecision of width measurements, or smaller numeric sampling, is unknown.

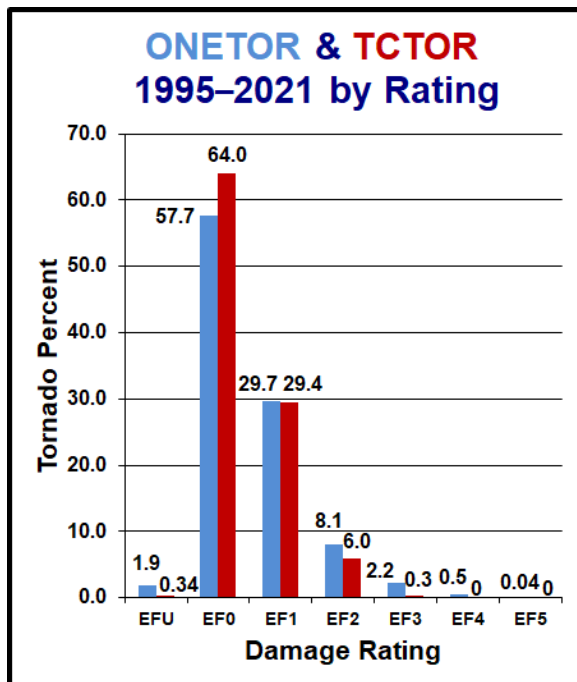


Figure 9. Percentage of ONETOR (light blue) and TCTOR (red) entries by damage rating for 1995–2021. EF stands for both F and EF ratings inclusively; however, no F-era tornadoes (pre-2007) were rated U (unknown).

g. Temporal distributions

Corresponding well to the frequency of midlatitude TC events in the U.S., the occurrence of TC tornadoes peaks in September (Fig. 14). That month alone had 47% of all TC tornadoes, with 70% in August and September combined (climatological peak months of landfalling U.S. TCs).

Though they have happened at all hours of day and night, TC tornadoes favor diurnal cycles, when CAPE maximizes in TC environments, especially inland (e.g., McCaul 1991; E12). Using 1200–2359 UTC as a coarse proxy for local day and night in the central and eastern U.S. (Fig. 15), 68% of TCTOR events have been during daytime. Consistent with E10, nocturnal TC tornadoes remained more common during the day of landfall than on later inland days. The sample size of significant tornadoes is relatively small (109 events, about 6% of TCTOR); of those, 70 (64%) fell in daytime bins. This is similar enough to the overall day/night distribution that no significant differences can be asserted. The only violent (F4) TC tornadoes on record, rated by Grazulis (1993), preceded TCTOR, and occurred at night in hurricanes Carla (1961) and Hilda (1964).

h. Variation from TC to TC

Tornado production can change greatly from TC to TC, as evident in Figs. 1 and 8, and Table 1. Nineteen TCs from 1995–2021 spawned just one recorded tornado each, in contrast to those profusely tornadic systems listed in Table 1. Duration of tornadic production varies greatly also, with Harvey of

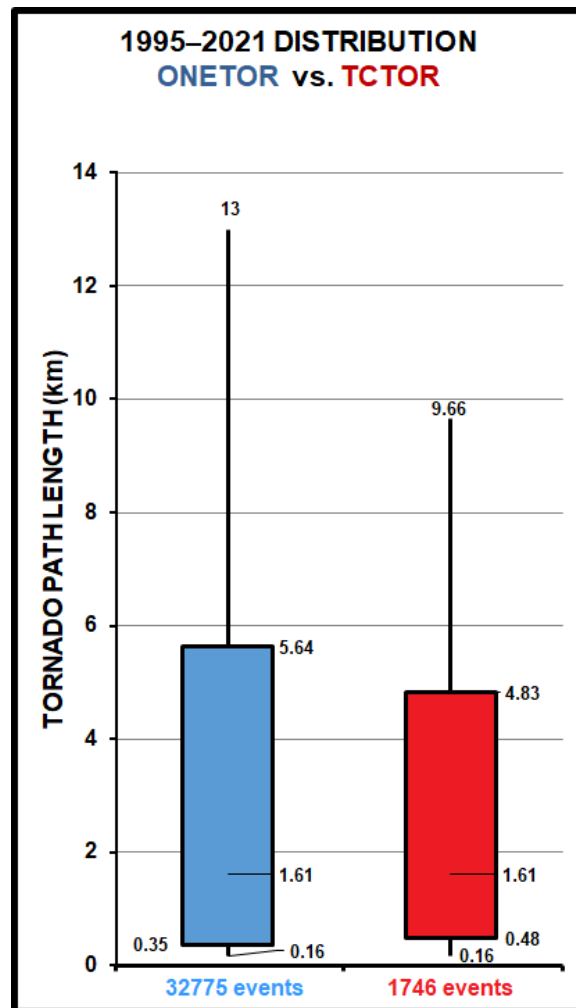


Figure 10. Boxplots of tornado path-length distributions (km) from 1995–2021: ONETOR (light blue) and TCTOR (red). Boxes represent 25<sup>th</sup> and 75<sup>th</sup> percentile with median bar, all labeled. Whisker ends reach to 10<sup>th</sup> and 90<sup>th</sup> percentiles. Sample sizes appear at bottom.

2017 yielding tornadoes in parts of a record seven consecutive local calendar days (eight straight UTC days). Mesoscale environmental variability within the TC envelope can alter tornado potential day to day, even hour to hour (e.g., Baker et al. 2009; Nowotarski et al. 2021). Therefore, despite the informative utility of climatology, *each TC's tornado threat should be treated operationally as its own individualized forecast challenge*, and diagnosed accordingly with all relevant analytic tools available to the forecast team.

4. SUMMARY and DISCUSSION

An updated version of the public-domain, E10 TCTOR database is described and analyzed, with 1746 documented TC tornadoes from 1995–2021 (609 to expand the dataset from 2010 onward). The year 1995 was chosen to start the climatology, given nearly simultaneous effective completion of the nationwide WSR-88D network, shifts in overall tornado warning, verification and documentation

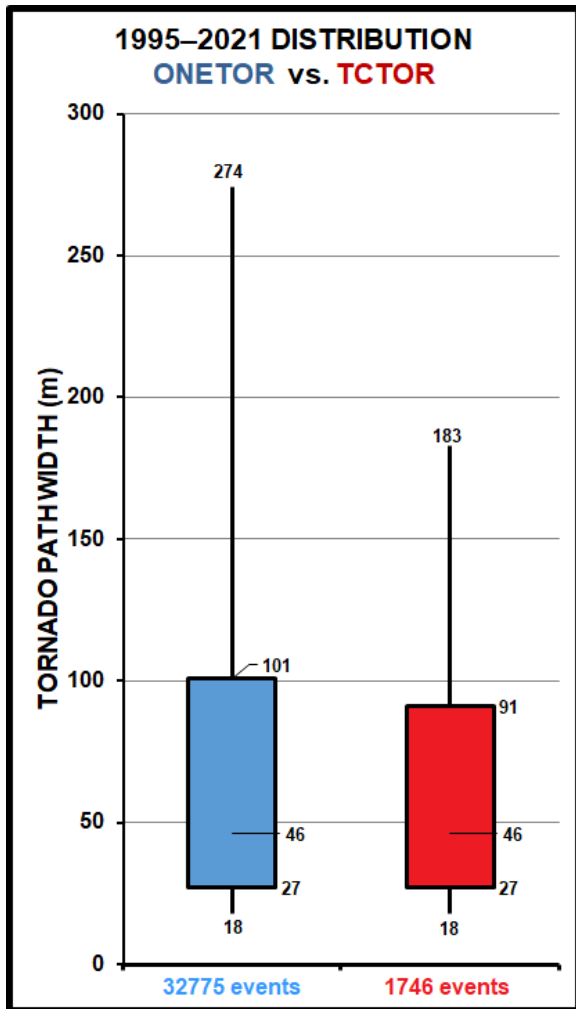


Figure 11: As in Fig. 10, but for path width (m).

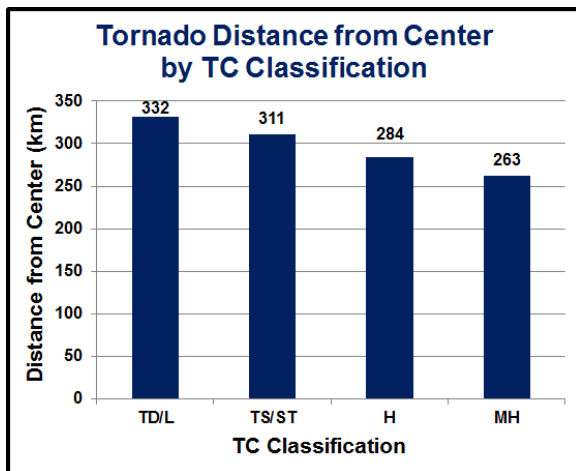


Figure 12: Mean tornado distance from TC center (km) by classification at tornado time (1995–2021). Bins are: TD/L (tropical depression and remnant low), TS/ST (tropical and subtropical storm), H (hurricane, categories 1–2), and MH (major hurricane, categories 3–5).

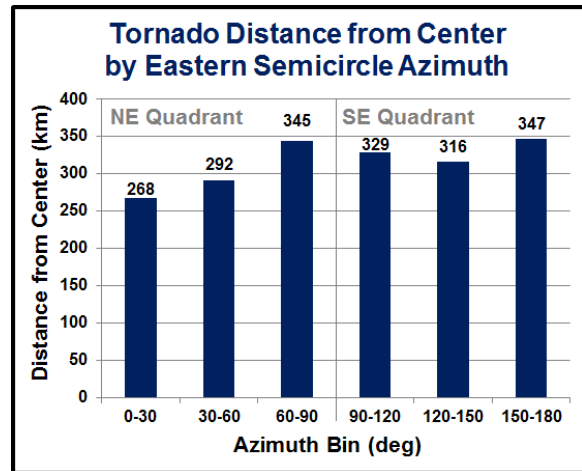


Figure 13: Mean TCTOR (1995–2021) tornado distance from TC center (km) by azimuthal bins (deg) within the eastern semicircle. Northeastern and southeastern quadrants are demarcated.

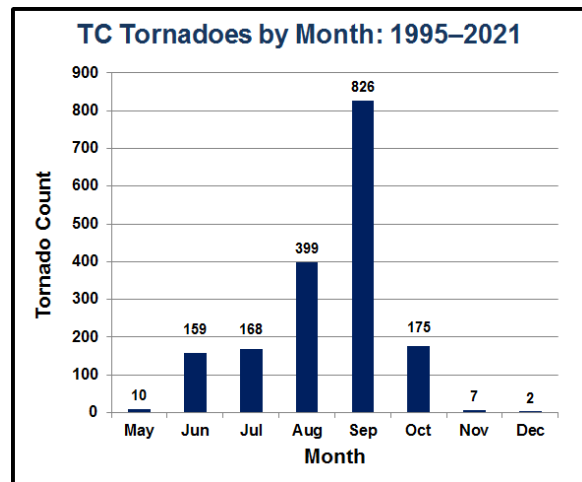


Figure 14: Total monthly occurrence of TCTOR events.

practices accompanying those radars, greater overall technological documentation capabilities, and change in the path-width standard. As in E10, the TCTOR data are gathered from ONETOR yearly after hurricane season, analyzed individually and meteorologically where any uncertainty may exist as to whether a tornado was produced by a TC, and quality-controlled for errors common to ONETOR (Edwards et al. 2012b, 2022).

Analyses largely confirm and reinforce climatological results from E10 and previous work described in the text body, including the tendency for most TC tornadoes to occur within  $\approx 700$  km north through southeast of center, within  $\approx 500$  km of the coastline, more diurnally than nocturnally, and at all stages of TC classification. Tornado occurrence generally expands radially outward as azimuth angle increases from due north to south-southeast, and as TC intensity diminishes. With a larger sample, the geographic coverage of TC tornadoes has expanded somewhat over inland areas, and now spans from

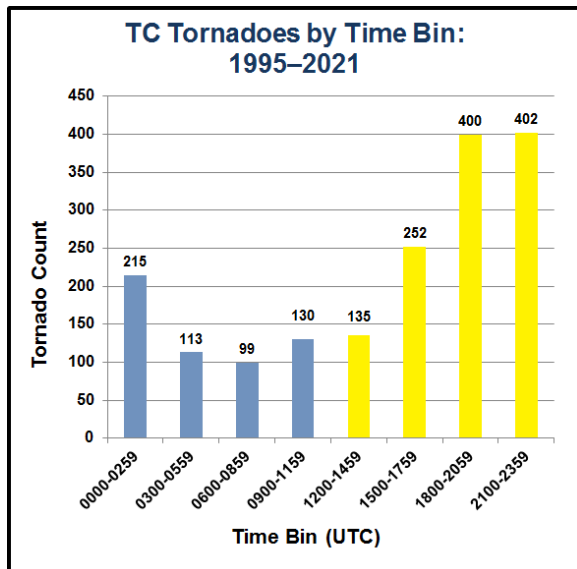


Figure 15. TCTOR events by 3-hourly UTC time bins as labeled. Golden bars represent the approximate local daytime cycle; blue represents approximate local night.

Oklahoma to the Ohio Valley States and New England. Damage rating, path width and path length are smaller overall for TC tornadoes than their non-TC counterparts, especially in the upper parts of the distributions. Extreme widths  $\geq 1000$  yd (914 m) and lengths  $\geq 52$  mi (83.7 km) that sometimes appear in ONETOR are absent from the TCTOR record, as are F/EF4–5 ratings (again note that two F4 TC tornadoes occurred in the 1960s; Grazulis 1993).

The dataset has been, and will be, revised for cases where errors or newly documented events are discovered, and/or reanalysis shows an existing record was either nontornadic or not within a TC envelope. As such, TCTOR is flexible, and may vary from previous years' versions. Corrections and other amendments to TCTOR are passed to ONETOR and *Storm Data* for updating in those datasets as well. To document such changes, a plain-text file accompanies the data, and both now are available via the informal section of the [SPC Publications website](#). Mosier and Edwards (2022, this conference) also present [an interactive-web-based viewer for TCTOR data](#) that likewise is updated annually, once the data itself are available and processed. Figures 6–8 were built using this new tool.

## ACKNOWLEDGMENTS

This documentation began as a planned quarter-century retrospective and examination of modern-era TC tornadoes, expanded to 27 years by pandemic-related delays to the AMS Severe Local Storms Conference. Great gratitude goes to successive SPC Warning Coordination Meteorologists Dan McCarthy, Greg Carbin, Patrick Marsh, and Matt Elliott, for their management, provision, successive improvements to, and quality control of the parent ONETOR data, and their flexibility in fixing ONETOR errors found in the TCTOR quality-control (QC) process. NHC supplied the six-hourly HURDAT points used to determine

center- and motion-relative tornado positions. The SPC Science Support Branch provided hardware and software platforms for TCTOR compilation, as well as archived surface and upper-air information for analyzing individual cases. Additional surface, upper-air and satellite imagery for QC came from archives at Plymouth State University, NESDIS and NCEI. NCEI and Amazon Web Services also supplied level-2 WSR-88D data for case examinations as necessary.

These scientists (in alphabetic order) have contributed helpful discussions, corrections, imagery, and/or additional data over the lifespan of TCTOR: Mike Brennan, George Bryan, Dereka Carroll-Smith, Daniel Cecil, Ariel Cohen, Lon Curtis, Andy Dean, Matt Eastin, Matt Elliott, Tom Grazulis, Bart Hagemeyer, E. W. (Bill) McCaul, Chris Nowotarski, Scott Overpeck, Joey Picca, Thea Sandmael, Al Sandrik, Ben Schenkel, David Schultz, Lori Schultz, Virginia Silvis, Bryan Smith, Justin Spotts, Rich Thompson, Stan Trier, Steve Weiss, and Gary Woodall. Israel Jirak (SPC) offered beneficial review of this paper.

## REFERENCES

- Baker, A. K., M. D. Parker, and M. D. Eastin, 2009: Environmental ingredients for supercells and tornadoes within Hurricane Ivan. *Wea. Forecasting*, **24**, 223–244.
- Brooks, H. E., 2004: On the relationship of tornado path length and width to intensity. *Wea. Forecasting*, **19**, 310–319.
- Carroll-Smith, D. L., L. C. Dawson, and R. J. Trapp, 2019: High-resolution real-data WRF modeling and verification of tropical cyclone tornadoes associated with Hurricane Ivan (2004). *Electronic J. Severe Storms Meteor.*, **14** (2), 1–36.
- , R. J. Trapp, and J. M. Done, 2021: Exploring inland tropical cyclone rainfall and tornadoes under future climate conditions through a case study of Hurricane Ivan. *J. Appl. Meteor. Clim.*, **60**, 103–118.
- Case, R. A., 1986: Atlantic hurricane season of 1985. *Mon. Wea. Rev.*, **114**, 1390–1405.
- Doswell, C. A. III, 1987: The distinction between large-scale and mesoscale contribution to severe convection: A case study example. *Wea. Forecasting*, **2**, 3–16.
- , 2007: Small sample size and data quality issues illustrated using tornado occurrence data. *Electronic J. Severe Storms Meteor.*, **2** (5), 1–16.
- , and D. W. Burgess, 1988: On some issues of United States tornado climatology. *Mon. Wea. Rev.*, **116**, 495–501.
- , H. E. Brooks, and N. Dotzek, 2009: On the implementation of the enhanced Fujita scale in the USA. *Atmos. Res.*, **93**, 554–563.



- Eastin, M. D., and M. C. Link, 2009: Miniature supercells in an offshore outer rainband of Hurricane Ivan (2004). *Mon. Wea. Rev.*, **137**, 2081–2104.
- Edwards, R., 1998: Storm Prediction Center support for landfalling tropical cyclones. Preprints, *23<sup>rd</sup> Conf. on Hurricanes and Tropical Meteor.*, Dallas, TX, Amer. Meteor. Soc., 53–56.
- , 2010: Tropical cyclone tornado records for the modernized NWS era. Preprints, *25<sup>th</sup> Conf. on Severe Local Storms*, Denver CO, Amer. Meteor. Soc., P3.1.
- , 2012: Tropical cyclone tornadoes: A review of knowledge in research and prediction. *Electronic J. Severe Storms Meteor.*, **7** (6), 1–61.
- , and A. E. Pietrycha, 2006: Archetypes for surface baroclinic boundaries influencing tropical cyclone tornado occurrence. Preprints, *23<sup>rd</sup> Conf. on Severe Local Storms*, St. Louis, MO, Amer. Meteor. Soc., P8.2.
- , and J.C. Picca, 2016: Tornadic debris signatures in tropical cyclones. Proc., *28<sup>th</sup> Conf. on Severe Local Storms*, Portland, OR, P162.
- , A. R. Dean, R. L. Thompson, and B. T. Smith, 2012a: Nonsupercell tropical cyclone tornadoes: Documentation, classification and uncertainties. Proc., *26<sup>th</sup> Conf. on Severe Local Storms*, Nashville TN, 9.6.
- , —, —, and —, 2012b: Convective modes for significant severe thunderstorms in the contiguous United States. Part III: Tropical cyclone tornadoes. *Wea. Forecasting*, **27**, 1507–1519.
- , J. G. LaDue, J. T. Ferree, K. Scharfenberg, C. Maier, and W. L. Coulbourne, 2013: Tornado intensity estimation: Past, present, and future. *Bull. Amer. Meteor. Soc.*, **94**, 641–653.
- , G. W. Carbin, and S. F. Corfidi, 2015: Overview of the Storm Prediction Center. Proc., *13<sup>th</sup> History Symp.*, Phoenix, AZ, Amer. Meteor. Soc., 1.1.
- , C. J. Nowotarski, S. Overpeck, and G. R. Woodall, 2018: Tornadoes in Hurricane Harvey: Documentation and environmental analysis. Proc., *29<sup>th</sup> Conf. on Severe Local Storms*, Stowe, VT, P52.
- , H. E. Brooks, and H. Cohn, 2021: Changes in tornado climatology accompanying the enhanced Fujita scale. *J. Appl. Meteor. Clim.*, **60**, 1465–1481.
- , M. S. Elliott, P. T. Marsh, and D. A. Speheger, 2022: Errors, oddities and artifacts in U.S. tornado data, 1995–2020. Proc., *30<sup>th</sup> Conf. on Severe Local Storms*, Amer. Meteor. Soc., Santa Fe, NM, 8.3B.
- Fujita, T. T., 1971: Proposed characterization of tornadoes and hurricanes by area and intensity. University of Chicago SMRP Research Paper 91, 42 pp.
- , 1981: Tornadoes and downbursts in the context of generalized planetary scales. *J. Atmos. Sci.*, **38**, 1511–1534.
- Grazulis, T. P., 1993: *Significant Tornadoes, 1680-1991*. Environmental Films, St. Johnsbury, VT, 1326 pp.
- Hales, J. E. Jr., 1988: Improving the watch/warning program through use of significant event data. Preprints, *15<sup>th</sup> Conf. on Severe Local Storms*, Baltimore, MD, Amer. Meteor. Soc., 165–168.
- Hill, E. L., W. Malkin and W. A. Schulz Jr., 1966: Tornadoes associated with cyclones of tropical origin—practical features. *J. Appl. Meteor.*, **5**, 745–763.
- Johns, R. H., and C. A. Doswell III, 1992: Severe local storms forecasting. *Wea. Forecasting*, **7**, 588–612.
- Knapp, K. R., M. C. Kruk, D. H. Levinson, H. J. Diamond, and C. J. Neumann, 2010: The International Best Track Archive for Climate Stewardship (IBTrACS) unifying tropical cyclone data. *Bull. Amer. Meteor. Soc.*, **91**, 363–376.
- Landsea, C. W., and J. L. Franklin, 2013: Atlantic hurricane database uncertainty and presentation of a new database format. *Mon. Wea. Rev.*, **141**, 3576–3592.
- McCaul, E. W., Jr., 1991: Buoyancy and shear characteristics of hurricane-tornado environments. *Mon. Wea. Rev.*, **119**, 1954–1978.
- Molinari, J., and D. Vollaro, 2010: Distribution of helicity, CAPE, and shear in tropical cyclones. *J. Atmos. Sci.*, **67**, 274–284.
- Moore, T. W., and R. W. Dixon, 2012: Tropical cyclone-tornado casualties. *Nat. Hazards*, **61**, 621–634.
- Mosier, R. M., and R. Edwards, 2022: Visualization tools for the Storm Prediction Center's tropical cyclone tornado database. Proc., *30<sup>th</sup> Conf. on Severe Local Storms*, Amer. Meteor. Soc., Santa Fe, NM, P172.
- Novlan, D. J., and W. M. Gray, 1974: Hurricane-spawned tornadoes. *Mon Wea Rev.*, **102**, 476–488.
- Nowotarski, C.J., J. Spotts, R. Edwards, S. Overpeck, and G.R. Woodall, 2021: Tornadoes in Hurricane Harvey. *Wea. Forecasting*, **36**, 1589–1609.
- Orton, R., 1970: Tornadoes associated with hurricane Beulah on September 19–23, 1967. *Mon Wea Rev.*, **98**, 541–547.
- Paredes, M., B. A. Schenkel, R. Edwards, and M. C. Coniglio, 2021: Tropical cyclone outer size

- impacts the number and location of tornadoes. *Geophys. Res. Lett.*, **48**, e2021GL095922.
- Pearson, A. D., and A. F. Sadowski, 1965: Hurricane-induced tornadoes and their distribution. *Mon. Wea. Rev.*, **93**, 461–464.
- Schaefer, J. T., and R. Edwards, 1999: The SPC tornado/severe thunderstorm database. Preprints, *11th Conf. on Applied Climatology*, Dallas, TX, Amer. Meteor. Soc., 6.11.
- Schneider, D., and S. Sharp, 2007: Radar signatures of tropical cyclone tornadoes in central North Carolina. *Wea. Forecasting*, **22**, 278–286.
- Schenkel, B. A., R. Edwards, and M. C. Coniglio, 2020: A climatological analysis of ambient deep-tropospheric vertical wind shear impacts upon tornadoes in tropical cyclones. *Wea. Forecasting*, **35**, 2033–2059.
- Schott, T. J., and Coauthors, cited 2022: The Saffir–Simpson hurricane wind scale. NOAA/National Weather Service. [Available online at <http://www.nhc.noaa.gov/sshws.shtml>.]
- Schultz, L. A., and D. J. Cecil, 2009: Tropical cyclone tornadoes, 1950–2007. *Mon. Wea. Rev.*, **137**, 3471–3484.
- Simpson, R. H., 1974: The hurricane disaster potential scale. *Weatherwise*, **27**, 169–186.
- Spratt, S. M., D. W. Sharp, P. Welsh, A. C. Sandrik, F. Alsheimer and C. Paxton, 1997: A WSR-88D assessment of tropical cyclone outer rainband tornadoes. *Wea. Forecasting*, **12**, 479–501.
- , B. C. Hagemeyer and D. W. Sharp, 2008: Treating hurricanes as mesoscale convective systems—A paradigm shift for WFO landfall operations. Preprints, *28th Conf. on Hurricanes and Tropical Meteorology*, Amer. Meteor. Soc., Orlando, FL, 11C.7.
- Thompson, R. L., and M. D. Vescio, 1998: The Destruction Potential Index: A method for comparing tornado days. Preprints, *19th Conf. on Severe Local Storms*, Minneapolis, MN, Amer. Meteor. Soc., 280–282.
- Thorne, P. W., and R. S. Vose, 2010: Reanalysis suitable for characterizing long-term trends: Are they really achievable? *Bull. Amer. Meteor. Soc.*, **91**, 353–361.
- Torn, R. D., and C. Snyder, 2013: Uncertainty in tropical cyclone best-track information. *Wea. Forecasting*, **27**, 715–729.
- Verbout, S. M., H. E. Brooks, L. M. Leslie, and D. M. Schultz, 2006: Evolution of the U.S. tornado database: 1954–2003. *Wea. Forecasting*, **21**, 86–93.
- , D. M. Schultz, L. M. Leslie, H. E. Brooks, D. J. Karoly and K. L. Elmore, 2007: Tornado outbreaks associated with landfalling hurricanes in the North Atlantic Basin: 1954–2004. *Meteor. Atmos. Phys.*, **97**, 1–4, doi: 10.1007/s00703-006-0256-x.
- Weiss, S. J., 1987: Some climatological aspects of forecasting tornadoes associated with tropical cyclones. Preprints, *17th Conf. on Hurricanes and Tropical Meteor.*, Miami, FL, Amer. Meteor. Soc., 160–163.